This article has been accepted for inclusion in a future issue of this journal. Content is final as presented, with the exception of pagination.

A Stochastic Distribution System Market Clearing and Settlement Model With Distributed Renewable Energy Utilization Constraints

Josue Campos do Prado, *Member, IEEE*, and Wei Qiao, *Fellow, IEEE*

***Abstract*—The increasing integration of distributed generation (DG) has changed the way modern power systems are planned and operated. However, new market mechanisms at the retail level are still needed to effectively integrate energy resources and emerging market participants in the distribution grid. In this article, a stochastic market clearing and settlement model with distributed renewable energy (DRE) utilization constraints is presented. The proposed model considers the uncertainties associated with the DRE productions in the distribution grid and ensures that a certain portion of the total available DRE at a specified time will be utilized with a high probability. The problem is formulated as a chance-constrained two-stage stochastic programming model that minimizes the expected distribution system operation cost and is solved through a sample average approximation algorithm. Case studies are conducted to verify the effectiveness of the proposed model for different DRE utilization requirements.**

***Index Terms*—Chance-constrained optimization, distributed energy resource (DER), distribution system market, distribution system operator (DSO), market clearing.**

NOMENCLATURE

Indices and Sets

a	Index for the demand bid blocks from the flexible loads (FLs), running from 1 to N_a.
b	Index for the energy production blocks from the dispatchable distributed generation (DDG) units, running from 1 to N_b.
i, s	Index of iterations in the sample average approximation (SAA) algorithm.
j, n, m	Indexes for distribution network nodes.
k	Index of market participants, running from 1 to N_k.
nm, jn	Indexes for distribution network branches.
t	Index of time periods, running from 1 to N_t.
ω, Ω_N	Index and set of DRE scenarios, respectively, where ω runs from 1 to N_ω.
$\Omega_{d(n)}$	Set of the decedent nodes connected to node n.
$\Omega_{k(n)}$	Set of the market participants located at node n.
$\Omega_{p(n)}$	Set of the precedent nodes connected to node n.

Input Parameters and Constants

β, ε	DRE utilization parameters.
$\lambda^{d}_{t,k,a}$	Price of the ath demand bid block of market participant k during period t.
λ^{DA}_{t}	Day-ahead transmission locational marginal price (TLMP) during period t.
$\lambda^{\mathrm{DRD}}_{t,k}$	Downward reserve demand price of market participant k during period t.
$\lambda^{DRU}_{t,k}$	Upward reserve demand price of market participant k during period t.
$\lambda^{g}_{t,k,b}$	Price of the bth generation offering block of market participant k during period t.
$\lambda^{RD}_{t,k}$	Downward reserve generation price of market participant k during period t.
$\lambda^{RU}_{t,k}$	Upward reserve generation price of market participant k during period t.
$\lambda^{\mathrm{Shed}}_{t,n}$	Load shedding cost at node n during period t.
$\lambda^{\mathrm{Spill}}_{t,n}$	DRE spillage cost at node n during period t.
π_ω	Probability of scenario ω.
M	Large auxiliary constant.
N_i, N_s	Number of iterations in the SAA algorithm.
$P^{d\max}_{t,k,a}$	FL capacity of the ath bid block of market participant k during period t.
$P^{DRU\max}_{t,k}$	Upward reserve demand capacity limit of market participant k during period t.
$P^{\mathrm{DRD}\max}_{t,k}$	Downward reserve demand capacity limit of market participant k during period t.
$P^{g\max}_{t,k,b}$	DDG capacity of the bth offering block of market participant k during period t.
$P^{\max}_{nm}$	Maximum active power flow of branch nm.
$P^{\min}_{nm}$	Minimum active power flow of branch nm.
$P^{nfl}_{t,k}$	Nonflexible demand of market participant k during period t.
$P^{RD\max}_{t,k}$	Downward reserve generation capacity limit of market participant k during period t.
$P^{RU\max}_{t,k}$	Upward reserve generation capacity limit of market participant k during period t.
$Q^{\max}_{nm}$	Maximum reactive power flow of branch nm.

Manuscript received October 9, 2020; revised January 25, 2021; accepted March 20, 2021. This work was supported in part by the U.S. National Science Foundation under CAREER Award ECCS-0954938, in part by the Nebraska Public Power District through the Nebraska Center for Energy Sciences Research, and in part by the Brazilian National Council for Scientific and Technological Development (CNPq). *(Corresponding author: Wei Qiao.)*

Josue Campos do Prado is with the School of Engineering and Computer Science, Washington State University Vancouver, Vancouver, WA 98686 USA (e-mail: josue.camposdoprado@wsu.edu).

Wei Qiao is with the Power and Energy Systems Laboratory, Department of Electrical and Computer Engineering, University of Nebraska-Lincoln, Lincoln, NE 68588-0511 USA (e-mail: wqiao3@unl.edu).

Digital Object Identifier 10.1109/JSYST.2021.3068719

1937-9234 © 2021 IEEE. Personal use is permitted, but republication/redistribution requires IEEE permission.
See https://www.ieee.org/publications/rights/index.html for more information.

Authorized licensed use limited to: University of Nebraska - Lincoln. Downloaded on July 19,2021 at 19:01:47 UTC from IEEE Xplore. Restrictions apply.

This article has been accepted for inclusion in a future issue of this journal. Content is final as presented, with the exception of pagination.

$Q_{nm}^{\min}$ Minimum reactive power flow of branch *nm*.
r_{jn} Resistance of branch *jn*.
$V_n^{\max}$ Maximum squared voltage magnitude at node *n*.
$V_n^{\min}$ Minimum squared voltage magnitude at node *n*.
x_{jn} Reactance of branch *jn*.

Random Variables

$P_{t,n,\omega}^{\mathrm{DRE}}$ DRE production at node *n* during period *t* and scenario ω.

Decision Variables – First Stage

$E_{t,k}$ Power sold, if positive, or purchased, if negative, by the market participant *k* during period *t* in the first stage.
$P_{t,nm}$ Active power flow of branch *nm* during period *t*.
$P_{t,k,a}^{d}$ Power awarded to the *a*th demand bid block of market participant *k* during period *t*.
P_t^{DA} Amount of power purchased in the day-ahead wholesale market by the distribution system operator (DSO) during period *t*.
$P_{t,k}^{DRD}$ Downward FL reserve capacity of market participant *k* during period *t*.
$\bar{P}_{t,n}^{\mathrm{DRE}}$ Amount of DRE scheduled by the DSO at node *n* during period *t* in the first stage.
$P_{t,k}^{DRU}$ Upward FL reserve capacity of market participant *k* during period *t*.
$P_{t,k,b}^{g}$ Power awarded to the *b*th generation offering block of market participant *k* during period *t*.
$P_{t,k}^{RD}$ Downward DDG reserve capacity of market participant *k* during period *t*.
$P_{t,k}^{RU}$ Upward DDG reserve capacity of market participant *k* during period *t*.
Q_t Reactive power at the substation during period *t*.
$Q_{t,nm}$ Reactive power flow of branch *nm* during period *t*.
$V_{t,n}$ Squared voltage magnitude at node *n* and period *t*.
$\lambda_{t,n}^{P}$ Lagrange multiplier associated with the power balance constraint of node *n* during period *t* in the first stage.
$z_{t,\omega}$ Auxiliary binary variable used to convert the nonlinear DRE utilization constraint for time *t* and scenario ω into a set of linear constraints.

Decision Variables – Second Stage

$p_{t,nm,\omega}$ Altered active power flow of branch *nm* in the second stage during period *t* and scenario ω.
$p_{t,k,\omega}^{DRD}$ Downward FL reserve capacity of market participant *k* deployed in the second stage during period *t* and scenario ω.
$p_{t,k,\omega}^{DRU}$ Upward FL reserve capacity of market participant *k* deployed in the second stage during period *t* and scenario ω.
$p_{t,k,\omega}^{RD}$ Downward DDG reserve capacity of market participant *k* deployed in the second stage during period *t* and scenario ω.
$p_{t,k,\omega}^{RU}$ Upward DDG reserve capacity of market participant *k* deployed in the second stage during period *t* and scenario ω.
$p_{t,k,\omega}^{\mathrm{Shed}}$ Total load shedding of market participant *k* during period *t* and scenario ω.
$p_{t,n,\omega}^{\mathrm{Spill}}$ Total DRE spillage at node *n* during period *t* and scenario ω.
$q_{t,nm,\omega}$ Altered reactive power flow of branch *nm* in the second stage during period *t* and scenario ω.
$S_{t,k,\omega}$ Revenue or cost of market participant *k* during period *t* and scenario ω.
$v_{t,n,\omega}$ Altered squared voltage magnitude at node *n* in the second stage during period *t* and scenario ω.
$\varphi_{t,n,\omega}$ Lagrange multiplier associated with the power balance constraint of node *n* during period *t* and scenario ω in the second stage.
$\Delta E_{t,k,\omega}$ Power sold, if positive, or purchased, if negative, by the market participant *k* during period *t* and scenario ω in the second stage.

Abbreviations

DDG Dispatchable distributed generation.
DER Distributed energy resource.
DG Distributed generation.
DLMP Distribution locational marginal price.
DRE Distributed renewable energy.
DRFL Downward reserve from flexible loads.
DRPG Downward reserve from dispatchable distributed generation units.
DSE Distributed solar energy.
DSO Distribution system operator.
EDSE Energy from distributed solar energy units.
EFL Energy from fixed loads.
FL Flexible load.
NFL Nonflexible load.
SAA Sample average approximation.
URFL Upward reserve from flexible loads.
URPG Upward reserve from dispatchable distributed generation units.
U.S. United States.

I. Introduction

POWER systems around the world are undergoing significant transformations as they move toward increasing decarbonization, decentralization, and digitalization. The European Union, for example, is committed to reducing greenhouse gas emissions by 40% compared to 1990 levels by 2030 [1]. In the United States (U.S.), California, New Jersey, and New York have set goals to generate 50% of their electricity from renewable resources by 2030 [2]. One example of the move toward decentralization is the increasing adoption of distributed energy resources (DERs), which is impacting the electricity sector in several ways and contributing to increased power system reliability, resilience, and sustainability. In 2017, different classes of DERs provided over 45 GW of flexible capacity on the U.S. summer peak. By 2023, DERs are expected to provide 104 GW of flexible capacity in the U.S., with nearly 45 GW provided by distributed solar energy (DSE) units [3]. In addition, the global DER capacity is expected to reach over 500 GW by 2028 [4].

Authorized licensed use limited to: University of Nebraska - Lincoln. Downloaded on July 19,2021 at 19:01:47 UTC from IEEE Xplore. Restrictions apply.

This article has been accepted for inclusion in a future issue of this journal. Content is final as presented, with the exception of pagination.

In the last few years, there have been many discussions on the creation of distribution system markets coordinated by distribution system operators (DSOs), which are envisioned as entities capable of operating the distribution network and coordinating the retail electricity market in neutral and transparent ways, similar to how independent system operators and regional transmission organizations operate the transmission grids and coordinate the wholesale electricity markets in the U.S [5]. However, DSOs are expected to facilitate the integration of DERs and reduce the dependency on centralized energy resources through decentralized electricity markets at the retail level. Technical and regulatory discussions on various DSO constructs that have been proposed in recent years are provided in [5]–[8].

Some market clearing and settlement mechanisms for DSOs have been recently presented in the literature. However, most of the existing models do not consider the uncertainties related to DERs. In [9], a simple market clearing and settlement mechanism comprising only fixed and flexible loads (FLs) was presented. The model in [9] was expanded in [10] and [11] to incorporate penalty-based pricing mechanisms. A distribution system energy auction considering flexible and fixed loads and distributed renewable energy (DRE) units was presented in [12]. However, that work assumed that all DRE units were supported by energy storage systems, thus neglecting the stochastic nature of DRE. In [13], a double-sided auction market mechanism for a distribution system market operator was presented. However, the market-clearing process was assumed to rely on DRE forecasts and, thus, may result in increased operational costs for the market operator when the DRE forecast errors are high. A market-clearing mechanism that incorporates Volt/VAR control and distribution network reconfiguration was proposed in [14]. However, all distributed generation (DG) outputs were assumed to be known. Other deterministic distribution system market-clearing models can be found in [15]–[24].

In contrast to the aforementioned deterministic distribution system market-clearing models, some recent works modeled the uncertainties related to the DERs in the DSO's decision model. In [25], a stochastic distribution system market framework considering the integration of electric vehicle aggregators was proposed. The work in [26] proposed a distribution system market clearing that modeled the uncertainties of DRE and a settling model based on energy and reserve capacity. However, that work did not consider reactive power and voltage limit constraints, and the management of DRE spillage and load shedding. A transactive day-ahead distribution market with variable generation in which the renewable energy uncertainty was modeled through the probability efficient point method was presented in [27]. However, that model did not consider the reserve determination, thus limiting the balancing actions only to generation and load curtailment, which may result in high operational costs. In [28], a chance-constrained distribution electricity pricing model under uncertainty was presented. However, all DRE units were assumed to be uncontrollable behind-the-meter units that do not participate directly in the market and cannot interact with DSOs. In addition, the chance constraints in [28] were used to model generation and voltage limits only, and the balancing actions were assumed to be provided only by controllable distributed generators.

TABLE I
COMPARISON OF THE PROPOSED MODEL WITH PREVIOUS APPROACHES

Reference	Formulation	DRE Uncertainty	GR	LR	DRE Utilization
[9]-[24]	Deterministic	No	No	No	No
[25]	Stochastic	No	No	No	No
[26]	Stochastic	Yes	Yes	Yes	No
[27]	Stochastic	Yes	No	No	No
[28]	Stochastic	Yes	Yes	No	No
Proposed Model	Stochastic	Yes	Yes	Yes	Yes

GR: Generation Reserve; LR: Load Reserve.

In the existing distribution market-clearing models, the DSO's decisions are solely based on the minimization of the system operational cost while the management of DRE is limited or inexistent. Thus, the existing models cannot be used in systems that have requirements for DRE utilizations to meet decarbonization targets or achieve other sustainability goals. Moreover, the traditional incentive mechanisms for renewable energy development, such as tax credits and rebates, can help governments and other organizations achieve only medium- and long-term sustainability goals. Therefore, a market mechanism capable of managing DRE utilization in lower time scales (e.g., day ahead) may help several regions achieve short-term goals.

This article presents a day-ahead distribution system market clearing and settlement model with DRE utilization constraints through a chance-constrained two-stage stochastic optimization approach. The DSO determines the power imports from the wholesale electricity market as well as the scheduling of energy and reserve capacity in the first stage, which is also denoted as the planning stage. In the second stage, balancing actions are performed by the DSO according to the DRE production realizations at each node of the distribution system. The second stage is also denoted as the balancing stage. The objective of the resulting decision-making model is to minimize the total operation cost of the system (i.e., the costs of the planning stage along with the expected costs of the second stage) while satisfying the prespecified DRE utilization requirements. A comparison of the proposed model with the state-of-the-art distribution system market-clearing models is provided in Table I.

The main contributions of this article are twofold as follows.

1) It determines the energy and reserve scheduling for generation and load units while considering the uncertainties associated with the DRE productions at different distribution system nodes, the power flow and voltage limits of the distribution network, and the management of DRE spillage and load shedding actions. Different from traditional market-clearing models that consider reserve provision from generating units only, the proposed model considers upward and downward reserve provisions from both generating units and FLs, thus increasing the demand response in the system.
2) It incorporates DRE utilization requirements, which are modeled as chance constraints, to ensure that a certain portion of the total available DRE in the system will be utilized with a high probability at a specified time. To

Authorized licensed use limited to: University of Nebraska - Lincoln. Downloaded on July 19,2021 at 19:01:47 UTC from IEEE Xplore. Restrictions apply.

This article has been accepted for inclusion in a future issue of this journal. Content is final as presented, with the exception of pagination.

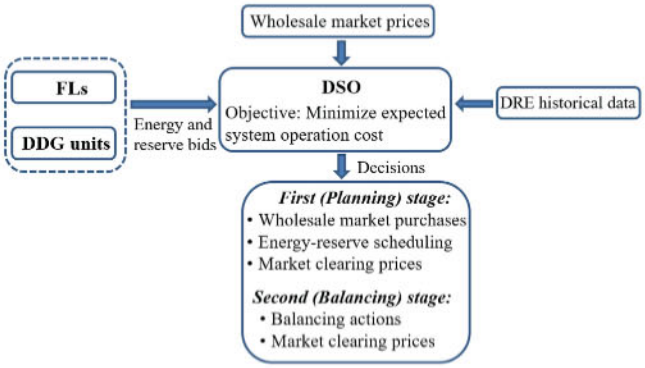

Fig. 1. Proposed problem framework.

the best of the authors' knowledge, no previous work has considered stochastic joint energy and reserve electricity market-clearing model with renewable energy utilization constraints at the wholesale or retail level.

The remainder of this article is organized as follows. Section II describes the main assumptions and the mathematical formulation of the proposed model. Section III describes the algorithm used to solve the resulting problem. In Section IV, case studies are performed, and the results are discussed. Finally, relevant conclusions are presented in Section V.

II. Problem Formulation

A. Assumptions

The proposed problem framework is illustrated in Fig. 1. Each FL and dispatchable distributed generation (DDG) unit is assumed to submit a demand bid and a generation offering curve, respectively, along with its upward and downward reserve capacities and prices for the next operating day to the DSO. Different from FLs, the nonflexible loads (NFLs) do not submit load bids to the DSO since they cannot be easily adjusted. NFLs are the only loads subject to load shedding. Moreover, the DSO is assumed to have knowledge of the expected value and the error distribution of DRE production at all distribution system nodes with DRE units.

After all curves and parameters are received by the DSO, the market is cleared and the amount of power purchased in the day-ahead wholesale market, the scheduling of energy and reserve, and the distribution locational marginal price (DLMPs) are determined. In this decision-making process, the balancing actions performed in the second stage are taken into account for several DRE production realizations. Such balancing actions include the real-time deployments of upward/downward reserve from FLs and DDG units along with DRE spillage and load shedding actions in every period t of the operating day.

B. Objective Function

The objective function of the proposed market clearing problem is formulated mathematically as follows:

$$\text{Minimize} \sum_{k=1}^{N_k}\left(P_t^{DA}\lambda_t^{DA}+\sum_{b=1}^{N_b}P_{t,k,b}^{g}\lambda_{t,k,b}^{g}-\sum_{a=1}^{N_a}P_{t,k,a}^{d}\lambda_{t,k,a}^{d}\right)$$
$$+\sum_{\omega=1}^{N_\omega}\sum_{k=1}^{N_k}\sum_{n\in\Lambda_{\text{DRE}}}\pi_\omega\left(p_{t,k,\omega}^{RU}\lambda_{t,k}^{RU}-p_{t,k,\omega}^{RD}\lambda_{t,k}^{RD}+p_{t,k,\omega}^{DRD}\lambda_{t,k}^{DRD}\right.$$
$$\left.-p_{t,k,\omega}^{DRU}\lambda_{t,k}^{DRU}+p_{t,n,\omega}^{\text{Spill}}\lambda_{t,n}^{\text{Spill}}+p_{t,k,\omega}^{\text{Shed}}\lambda_{t,k}^{\text{Shed}}\right). \quad (1)$$

The DSO's objective in (1) comprises two terms. The first term minimizes the total first-stage system operation cost, which is obtained through the scheduling of energy and reserve capacity with the maximum possible social welfare. Note that the DRE units are assumed to operate with zero marginal costs. The second term minimizes the expected total balancing cost in the second stage, which considers the deployment of upward and downward reserves from FLs and DDG units along with the costs associated with load shedding and DRE spillage.

C. Planning Stage Constraints

The constraints related to the planning stage are formulated mathematically as follows:

$$0\le P_{t,k,a}^{d}\le P_{t,k,a}^{d\max} \qquad \forall t,\ \forall k,\ \forall a \quad (2)$$
$$0\le P_{t,k,b}^{g}\le P_{t,k,b}^{g\max} \qquad \forall t,\ \forall k,\ \forall b \quad (3)$$
$$\sum_{a=1}^{N_a}P_{t,k,a}^{d}+P_{t,k}^{DRU}\le\sum_{a=1}^{N_a}P_{t,k,a}^{d\max} \qquad \forall t,\ \forall k \quad (4)$$
$$\sum_{a=1}^{N_a}P_{t,k,a}^{d}-P_{t,k}^{DRD}\ge 0 \qquad \forall t,\ \forall k \quad (5)$$
$$\sum_{b=1}^{N_b}P_{t,k,b}^{g}+P_{t,k}^{RU}\le\sum_{b=1}^{N_b}P_{t,k,b}^{g\max} \qquad \forall t,\ \forall k \quad (6)$$
$$\sum_{b=1}^{N_b}P_{t,k,b}^{g}-P_{t,k}^{RD}\ge 0 \qquad \forall t,\ \forall k \quad (7)$$
$$0\le P_{t,k}^{RU}\le P_{t,k}^{RU\max} \qquad \forall t,\ \forall k \quad (8)$$
$$0\le P_{t,k}^{RD}\le P_{t,k}^{RD\max} \qquad \forall t,\ \forall k \quad (9)$$
$$0\le P_{t,k}^{DRU}\le P_{t,k}^{DRU\max} \qquad \forall t,\ \forall k \quad (10)$$
$$0\le P_{t,k}^{DRD}\le P_{t,k}^{DRD\max} \qquad \forall t,\ \forall k \quad (11)$$
$$0\le \bar{P}_{t,n}^{DRE}\le \max\left(P_{t,n,\omega}^{DRE}\right) \qquad \forall t,\ \forall n \quad (12)$$
$$P_t^{DA}=\sum_{m\epsilon\Omega_{d(1)}}P_{t,1m} \qquad \forall t \quad (13)$$
$$Q_t=\sum_{m\epsilon\Omega_{d(1)}}Q_{t,1m} \qquad \forall t \quad (14)$$
$$\sum_{m\epsilon\Omega_{d(n)}}P_{t,nm}=\sum_{j\in\Omega_{p(n)}}P_{t,jn}+\bar{P}_{t,n}^{DRE}$$
$$+\sum_{k\in\Omega_{k(n)}}\left(\sum_{b=1}^{N_b}P_{t,k,b}^{g}-P_{t,k}^{nfl}-\sum_{a=1}^{N_a}P_{t,k,a}^{d}\right) \qquad \forall t,\ \forall n\ne 1 \quad (15)$$

Authorized licensed use limited to: University of Nebraska - Lincoln. Downloaded on July 19,2021 at 19:01:47 UTC from IEEE Xplore. Restrictions apply.

This article has been accepted for inclusion in a future issue of this journal. Content is final as presented, with the exception of pagination.

$$\sum_{m\in\Omega_{d(n)}} Q_{t,nm} = \sum_{j\in\Omega_{p(n)}} Q_{t,jn} + \sum_{k\in\Omega_{k(n)}} \left(\sum_{b=1}^{N_b} \gamma_n^g P_{t,k,b}^g - \gamma_n^{nfl} P_{t,k}^{nfl} - \sum_{a=1}^{N_a} \gamma_n^d P_{t,k,a}^d \right) + \gamma_n^{DRE} \bar{P}_{t,n}^{DRE} \; \forall t, \;\; \forall n \neq 1 \tag{16}$$

$$V_{t,n} = V_{t,j} - 2\left(r_{jn} P_{t,jn} + x_{jn} Q_{t,jn}\right) \;\; \forall t, \; \forall n, j \in \Omega_{p(n)} \tag{17}$$

$$V_n^{\min} \leq V_{t,n} \leq V_n^{max} \qquad \forall t, \; \forall n \tag{18}$$

$$P_{nm}^{\min} \leq P_{t,nm} \leq P_{nm}^{\max} \qquad \forall t, \; \forall nm \tag{19}$$

$$Q_{nm}^{\min} \leq Q_{t,nm} \leq Q_{nm}^{\max} \qquad \forall t, \; \forall nm \tag{20}$$

$$P_t^{DA} \geq 0 \; \forall t. \tag{21}$$

Constraints (2) and (3) limit the active power from FLs and DDG units, respectively, in each block. Constraints (4)–(7) enforce the mutual exclusivity of energy and reserve capacity provided by FLs and DDG units. Constraints (8)–(11) limit the upward and downward reserve capacities scheduled in the first stage. The DRE scheduled at each node is limited by the scenario with the highest DRE production in (12). Constraints (13)–(17) constitute the linearized DistFlow equations, which are widely used in the literature to model the voltage and power flow in the distribution network [29]–[31]. In particular, (13) and (14) constitute the active and reactive power balance at the substation, respectively. Note that γ_n^g, γ_n^{DRE}, γ_n^d, and γ_n^{nfl} are the coefficients used to convert the active power of the DDG units, DRE units, NFLs, and FLs, respectively, into their reactive power values [31]. Constraint (18), (19), and (20) limit the squared voltage magnitude at each node, the active power in each branch, and the reactive power in each branch, respectively. Constraint (21) ensures that the active power purchased from the wholesale market is non-negative.

Note that no reserve requirement constraint was included in (2)–(21) since the energy dispatch in the planning stage is determined by modeling the balancing actions in the second stage, as it will be described in Section II-E.

D. DRE Utilization Constraints

Chance-constrained optimization programs ensure that one or more constraints are satisfied with a prespecified probability. In this article, a DRE utilization policy is enforced to ensure that a certain portion of DRE is scheduled in the planning stage while keeping all the other system constraints. The DRE utilization is defined as the difference between the amount of DRE scheduled by the DSO in the planning stage, $\bar{P}_{t,n}^{DRE}$, and the actual DRE production in scenario ω, $P_{t,n,\omega}^{DRE}$. The following DRE utilization policy is considered [32]: For each period t of the clearing planning horizon, the DRE usage in the set of distribution system nodes with DRE, Λ_{DRE}, must be larger than or equal to β with a probability of at least $1-\varepsilon$, where $0 \leq \beta \leq 1$ and $\varepsilon \leq 1$. This policy can be mathematically expressed as follows [32]:

$$Pr\left[\sum_{n\in\Lambda_{DRE}} \left(\beta P_{t,n,\omega}^{DRE} - \bar{P}_{t,n}^{DRE}\right) \leq 0 \right] \geq 1-\varepsilon \; \forall t. \tag{22}$$

The nonlinear chance constraint (22) can be replaced by the equivalent linear constraints (23)–(25) by introducing binary variables $z_{t,\omega}$ and using the big-M method, where M is a sufficiently large auxiliary constant, to describe the same feasibility set in (22). More details on how to reformulate nonlinear chance constraints into linear expressions and choose the proper value of M can be found in [32] and [33], respectively.

$$\sum_{n\in\Lambda_{DRE}} \left(\beta P_{t,n,\omega}^{DRE} - \bar{P}_{t,n}^{DRE}\right) - M z_{t,\omega} \leq 0 \quad \forall t, \; \forall \omega \tag{23}$$

$$\sum_{\omega=1}^{N_\omega} z_{t,\omega} \leq N_\omega \varepsilon \qquad \forall t \tag{24}$$

$$z_{t,\omega} \in \{0,1\} \qquad \forall t, \; \forall \omega. \tag{25}$$

E. Balancing Stage Constraints

The constraints related to the balancing stage are formulated mathematically as follows:

$$\sum_{m\in\Omega_{d(n)}} P_{t,nm} - \sum_{j\in\Omega_{p(n)}} P_{t,jn} + \sum_{k\in\Omega_{k(n)}} (p_{t,k,\omega}^{RU} - p_{t,k,\omega}^{RD} + p_{t,k,\omega}^{DRD} - p_{t,k,\omega}^{DRU} + p_{t,k,\omega}^{Shed}) + P_{t,n,\omega}^{DRE} - \bar{P}_{t,n}^{DRE} - p_{t,n,\omega}^{Spill} = \sum_{m\in\Omega_{d(n)}} p_{t,nm,\omega} \qquad \forall t, \; \forall n, \; \forall \omega \tag{26}$$

$$\sum_{m\in\Omega_{d(n)}} Q_{t,nm} - \sum_{j\in\Omega_{p(n)}} Q_{t,jn} + \sum_{k\in\Omega_{k(n)}} [\gamma_n^g (p_{t,k,\omega}^{RU} - p_{t,k,\omega}^{RD}) + \gamma_n^d \left(p_{t,k,\omega}^{DRD} - p_{t,k,\omega}^{DRU}\right) + \gamma_n^{nfl} p_{t,k,\omega}^{Shed}] + \gamma_n^{DRE} (P_{t,n,\omega}^{DRE} - \bar{P}_{t,n}^{DRE} - p_{t,n,\omega}^{\text{Spill}}) = \sum_{m\in\Omega_{d(n)}} q_{t,nm,\omega} \; \forall t, \; \forall n, \; \forall \omega \tag{27}$$

$$v_{t,n,\omega} = v_{t,j,\omega} - 2\left(r_{jn} p_{t,jn,\omega} + x_{jn} q_{t,jn,\omega}\right) \qquad \forall t, \; \forall n, j \in \Omega_{p(n)}, \; \forall \omega \tag{28}$$

$$V_n^{\min} \leq v_{t,n,\omega} \leq V_n^{\max} \qquad \forall t, \; \forall n, \; \forall \omega \tag{29}$$

$$P_{nm}^{\min} \leq p_{t,nm,\omega} \leq P_{nm}^{\max} \qquad \forall t, \; \forall n, \; \forall \omega \tag{30}$$

$$Q_{nm}^{\min} \leq q_{t,nm,\omega} \leq Q_{nm}^{\max} \qquad \forall t, \; \forall n, \; \forall \omega \tag{31}$$

$$0 \leq p_{t,n,\omega}^{\text{Spill}} \leq P_{t,n,\omega}^{DRE} \qquad \forall t, \; \forall n, \; \forall \omega \tag{32}$$

$$0 \leq p_{t,k,\omega}^{\text{Shed}} \leq P_{t,k}^{nfl} \qquad \forall t, \; \forall k, \; \forall \omega \tag{33}$$

$$0 \leq p_{t,k,\omega}^{RU} \leq P_{t,k}^{RU} \qquad \forall t, \; \forall k, \; \forall \omega \tag{34}$$

$$0 \leq p_{t,k,\omega}^{RD} \leq P_{t,k}^{RD} \qquad \forall t, \; \forall k, \; \forall \omega \tag{35}$$

$$0 \leq p_{t,k,\omega}^{DRU} \leq P_{t,k}^{DRU} \qquad \forall t, \; \forall k, \; \forall \omega \tag{36}$$

$$0 \leq p_{t,k,\omega}^{\text{DRD}} \leq P_{t,k}^{\text{DRD}} \qquad \forall t, \; \forall k, \; \forall \omega. \tag{37}$$

Authorized licensed use limited to: University of Nebraska - Lincoln. Downloaded on July 19,2021 at 19:01:47 UTC from IEEE Xplore. Restrictions apply.

This article has been accepted for inclusion in a future issue of this journal. Content is final as presented, with the exception of pagination.

Constraints (26)–(28) represent the altered DistFlow model when balancing actions are performed. Constraint (29), (30), and (31) limit the altered squared voltage magnitude at each node, the altered active power in each branch, and the altered reactive power in each branch, respectively. The amounts of DRE spillage and load shedding are limited in (32) and (33), respectively. Finally, constraints (34)–(37) limit the deployed upward and downward reserves by the respective reserve capacity values obtained in the first stage.

The resulting market-clearing model given by (1)–(21), (23)–(25), and (26)–(37) is a mixed-integer linear programming problem. Note that the number of continuous variables depends on several factors, such as the number of scenarios, the number of bid and offering blocks, and the number of nodes with DRE production. However, the number of integer variables is equal to the number of scenarios. The proposed model is also known as a variable power market-clearing model since the amount of power purchased in the day-ahead market, P_t^{DA}, is a decision variable in the problem formulation [9].

F. Market Settlement

The Lagrange multipliers of the first-stage active power balance constraint (15), $\lambda_{t,n}^{P}$, and the second-stage active power balance constraint (26), $\varphi_{t,n,\omega}$, are used in the proposed market settlement mechanism. These are the dual variables of (15) and (26), respectively, when the integer variables are fixed to their respective optimal values. More specifically, $\lambda_{t,n}^{P}$ is the DLMP at node n in the period t, which represents the marginal cost of supplying the next increment of load [15]. Furthermore, $\varphi_{t,n,\omega}$ is used to calculate the balancing price at node n in scenario ω and period t. Let $n(k)$ be the node index for the market participant k. The energy-only market settlement, which aims to determine the cost or revenue of each market participant for each time period and scenario, is mathematically formulated as follows [26], [34]:

$$S_{t,k,\omega} = \lambda_{t,n(k)}^{P} E_{t,k} + \lambda_{t,n(k),\omega}^{B} \Delta E_{t,k,\omega} \tag{38}$$

$$\lambda_{t,n(k),\omega}^{B} = \frac{\varphi_{t,n(k),\omega}}{\pi_{\omega}} \tag{39}$$

note that $S_{t,k,\omega}$ in (38) represents the resulting cost, if negative, or revenue, if positive, of the market participant k. The market settlement given by (38) and (39) is denoted as an energy-only market settlement since it is only based on energy payments (i.e., $E_{t,k}$ and $\Delta E_{t,k,\omega}$) and does not include any reserve capacity costs [34].

III. Solution Algorithm

A sample average approximation (SAA)-based solution algorithm is designed to solve the proposed chance-constrained two-stage stochastic program. The SAA algorithm [32], [35] is useful for solving stochastic optimization problems with a large number of random variables (e.g., DRE productions at several nodes of a distribution system) with better tractability than the traditional methods based on large scenario trees. The SAA-based solution algorithm consists of generating DRE scenarios (i.e., samples from the DRE probability distribution) and determining the lower and upper bound estimates of the resulting objective function value [i.e., the total expected system operation cost given by (1)], and the resulting optimality gap for a given scenario set. As the number of scenarios approaches infinity, the optimality gap approaches zero. Thus, the SAA algorithm allows one to find the number of scenarios that result in an acceptable optimality gap.

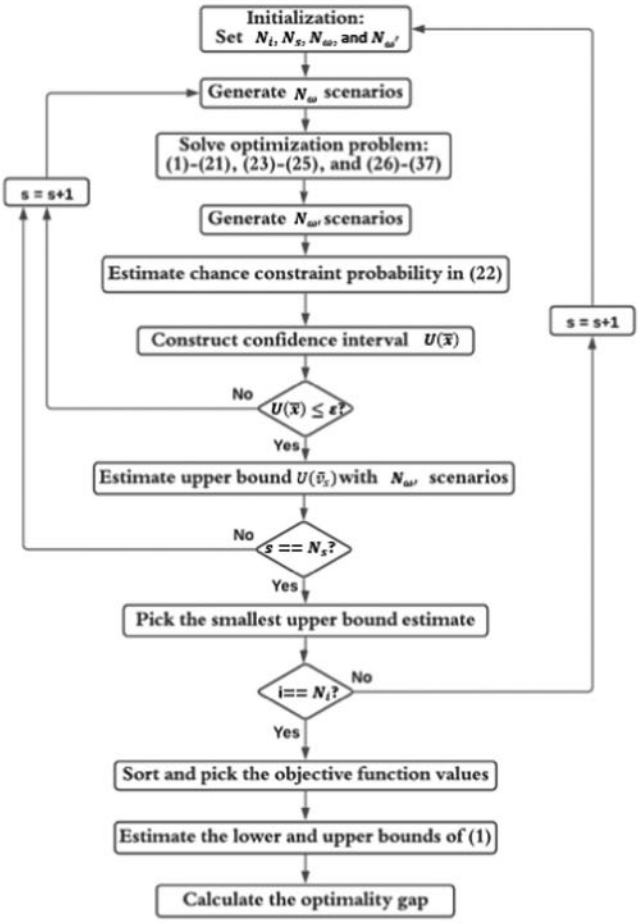

Fig. 2. Flowchart of the SAA algorithm for the proposed model.

Note that the second term of the objective function (1) minimizes the expected balancing cost, denoted as E[f(x_{Ω_N})], where x_{Ω_N} is the vector of the second-stage decisions for the uncertainty set Ω_N with N_ω scenarios. In the SAA framework, E[f(x_{Ω_N})] is reformulated as follows:

$$\mathrm{E}\left[\mathrm{f}\left(x_{\Omega_N}\right)\right] = \frac{1}{N_\omega} \sum_{\omega=1}^{N_\omega} \mathrm{f}\left(x_{\Omega_N}\right). \tag{40}$$

Different from the traditional methods based on large and fixed scenario trees, the SAA method allows calculation of the expected value of the balancing cost and verification of the quality of the solutions for scenarios sets of different sizes, which can be obtained by sampling a probability distribution.

The theoretical description (i.e., propositions, theorems, and proofs) of the SAA algorithm for chance-constrained optimization is provided in [35]. The main algorithm steps are summarized in Fig. 2 and described in detail as follows.

Authorized licensed use limited to: University of Nebraska - Lincoln. Downloaded on July 19,2021 at 19:01:47 UTC from IEEE Xplore. Restrictions apply.

This article has been accepted for inclusion in a future issue of this journal. Content is final as presented, with the exception of pagination.

1) Set the numbers of iterations N_i and N_s, the number of DRE scenarios N_ω of the set Ω_N to be tested, and the number of DRE scenarios $N_{\omega'}$ of the auxiliary validation set $\Omega_{N'}$, where $N_{\omega'} > N_\omega$.
2) For $i = 1, 2, \ldots, N_i$, repeat the following steps:
   2.1) For $s = 1, 2, \ldots, N_s$, repeat the following steps.
      a) Generate the scenario set $\Omega_N = \{\omega_1, \omega_2, \ldots, \omega_{N_\omega}\}$ with N_ω scenarios to be tested.
      b) Solve the proposed optimization problem given by (1)–(21), (23)–(25), and (26)–(37) to obtain the optimal first-stage solution $\bar{x}_s$ and the optimal objective function value in (1) as O_s.
      c) Generate the auxiliary validation scenario set $\Omega_{N'} = \{\omega'_1, \omega'_2, \ldots, \omega'_{N_{\omega'}}\}$ with $N_{\omega'}$ scenarios, where $N_{\omega'} > N_\omega$.
      d) Estimate the chance constraint probability in (22) as $\hat{q}_{N'}(\bar{x}_s)$ over the auxiliary validation set $\Omega_{N'}$ by

$$\hat{q}_{N'}(\bar{x}_s) = \Pr\{G(\bar{x}_s, \omega' \in \Omega_{N'}) > 0\} \quad (41)$$

      where G is the DRE utilization given in (22).
      e) Construct the 100 $(1-\tau)\%$ confidence interval upper bound on the chance constraint probability in (22), denoted as $U(\bar{x}_s)$, by

$$U(\bar{x}_s) = \hat{q}_{N'}(\bar{x}_s)\, z_\tau \sqrt{\frac{\hat{q}_{N'}(\bar{x}_s)\left(1 - \hat{q}_{N'}(\bar{x}_s)\right)}{N_{\omega'}}} \quad (42)$$

      where $z_\tau = \phi^{-1}(1-\tau)$ and ϕ is the cumulative distribution function of the standard normal distribution.
      f) If $U(\bar{x}_s) \le \varepsilon$, go to step (2.1.g; else, go back to step (2.1).
      g) Estimate the corresponding upper bound of the expected system operation cost with $N_{\omega'}$ DRE scenarios, denoted as $U(\bar{v}_s)$, by

$$U(\bar{v}_s) = c^T \bar{x}_s + \frac{1}{N_{\omega'}} \sum_{\omega'=1}^{N_{\omega'}} Q(\hat{x}_{\omega'}, \Omega_{N'}) \quad (43)$$

      where $Q(\hat{x}_{\omega'}, \Omega_{N'})$ is the second term of the objective function (1) with the second stage decisions $\hat{x}_{\omega'}$ and validation set $\Omega_{N'}$.
   2.2) Pick the smallest value of $U(\bar{v}_s)$ obtained in Step (2.1) and denote it as $\hat{g}^i$.
   2.3) Sort the N_s optimal objective function values obtained in Step (2.1.b) in nondecreasing order (i.e., $O_1 < O_2 < \ldots < O_{N_s}$). Let B denote the cumulative distribution function of a binomial distribution. Pick the Lth optimal value O_{L_s}, where L is the largest integer such that $B(L-1, \theta_{N_\omega}, N_s) \le \tau$, and $\theta_{N_\omega} = B(\varepsilon N_\omega, \varepsilon, N_\omega)$.

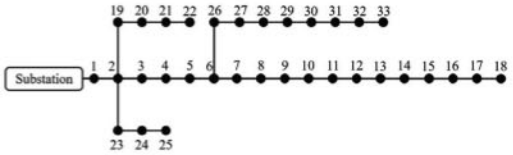

Fig. 3. The 33-node distribution system [31].

   3) Estimate the lower bound of the expected system operation cost $\bar{O}$ by

$$\bar{O} = \frac{1}{N_i} \sum_{i=1}^{N_i} O_{L_s}. \quad (44)$$

   4) Estimate the upper bound of the expected system operation cost $\hat{g}$ by

$$\hat{g} = \min_{1 \le i \le N_i} \hat{g}^i. \quad (45)$$

   5) Calculate the optimality gap as follows:

$$Gap = \frac{\left(\hat{g} - \bar{O}\right)}{\bar{O}}. \quad (46)$$

IV. Case Studies

A. Data

The proposed model is validated by using a 33-node and a 123-node distribution system. The systems are composed of DSE units, DDG units that provide energy only, DDG units that are capable of providing energy and upward/downward reserve, FLs that can provide reserve, FLs that cannot provide reserve, and NFLs. The DSO is assumed to participate in the Pennsylvania-Jersey-Maryland market [36]. The DSE production at each node is forecasted based on historical data from the National Solar Radiation Database [37] by using a seasonal autoregressive integrated moving average model in the MATLAB econometrics toolbox [38]. The DSE productions at all nodes are assumed to be uncorrelated. The DSE forecast errors are assumed to be normally distributed and equiprobable scenarios are generated from the resulting DSE distribution via Monte Carlo simulation to be used in the SAA algorithm described in Section III. Each time period t corresponds to one hour. A day with significant DSE production during hours 9–18 (i.e., from 09:00 AM to 06:00 PM) is considered. Additionally, the load shedding cost $\lambda_{t,n}^{Shed}$ is set to \$100/MWh for all nodes with NFLs; and the lower and upper voltage deviation limits with respect to the substation are set to –5% and +5%, respectively. The resulting optimization problem is solved by using Yalmip [39] and Gurobi 9.0 [40] in MATLAB. The computer used for simulation studies has a 4.60-Ghz, 4-core CPU, and a 16-GB RAM.

B. Results – 33-Node System

The 33-node distribution system is shown in Fig. 3. The DSE producers are located at nodes 4, 11, 17, 22, 25, and 33. A complete list of all agents in each node of the system and their respective energy and reserve price bids can be found in [41].

Authorized licensed use limited to: University of Nebraska - Lincoln. Downloaded on July 19,2021 at 19:01:47 UTC from IEEE Xplore. Restrictions apply.

This article has been accepted for inclusion in a future issue of this journal. Content is final as presented, with the exception of pagination.

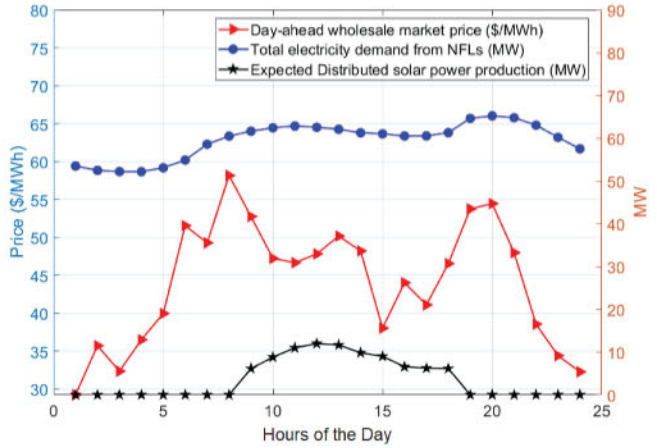

Fig. 4. Expected DSE production, wholesale market prices, and electricity demand from NFLs.

TABLE II
OPTIMALITY GAPS AND SIMULATION TIMES FOR DIFFERENT NUMBERS OF DRE SCENARIOS – 33-NODE SYSTEM

$(N_i, N_s, N_{\omega'})$	N_ω	Optimality Gap (%)	Solution Time (s)	Verification Time (s)
(5,5,1500)	10	1.79	0.7	217
	50	0.78	0.9	222
	100	0.55	1.7	243
	200	0.28	5.7	325
	300	0.13	9.9	425

TABLE III
TOTAL ENERGY AND RESERVE AMOUNTS (MWH) SCHEDULED IN THE PLANNING STAGE – 33-NODE SYSTEM

EG	EFL	EDSE	URPG	URFL	DRPG	DRFL
152.6	400.5	82.7	15.9	16.5	15.9	16.4

Fig. 4 shows the total expected DSE production in the system, the day-ahead wholesale market prices, and the electricity demand from NFLs for the operating day considered. Initially, the DSE spillage cost $\lambda_{t,n}^{Spill}$ is assumed to be \$25/MWh at all nodes with DSE production, and the chance-constraint parameters are $\beta = 0.8$ and $\varepsilon = 0.15$.

Table II shows the optimality gap, the solution time (i.e., the time to solve the problem using N_ω scenarios in Step (2.1.b) of the SAA algorithm), and the verification time (i.e., the time to calculate the optimality gap) for N_ω from 10 to 300. Note that the optimality gaps decrease and the simulation times increase as the size of the scenario set used in the SAA algorithm increases. An optimality gap lower than 0.15% was obtained with $(N_i, N_s, N_{\omega'}) = (5, 5, 1500)$ and $N_\omega = 300$, for a 95% confidence interval (i.e., $\tau = 0.05$).

Table III gives the total amounts of energy scheduled from the DDG units, FLs (EFL), and DSE units (EDSE) as well as the amounts of upward reserve from DDG units (URPG), FLs (URFL), and the downward reserve amounts from DDG units (DRPG), and FLs (DRFL), in the planning stage obtained with the proposed model. The amounts of upward and downward reserve are limited by the lowest and highest DRE production scenarios, respectively. In this case study, both reserve amounts

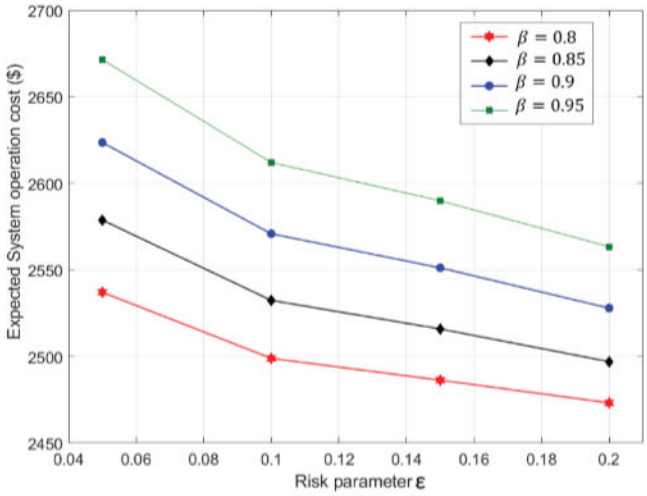

Fig. 5. System operation cost in the 12th hour for different values of ε and β.

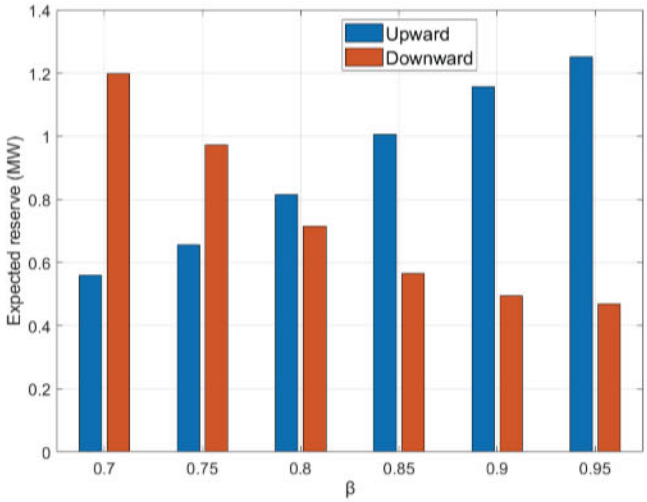

Fig. 6. Expected reserve deployed in the balancing stage in the 12th hour.

are nearly 40% of the total energy scheduled from DSE units, as shown in Table III.

The impact of different DRE utilization parameters ε and β on the expected system operation cost in the period with the highest DRE production (i.e., the 12th hour) is shown in Fig. 5. For a fixed risk parameter ε, the higher the value of β, the higher the system operation cost. On the other hand, for a fixed value of β, the higher the risk parameter ε, the lower the system operation cost. Thus, to minimize the operation cost of the system, one should choose the largest possible value for ε and the smallest possible value for β.

Fig. 6 shows the expected deployment of downward and upward reserves in the balancing stage in the 12th hour when ε is fixed to 0.2 and β is varied from 0.7 to 0.95. It turns out that the expected upward reserve deployed in the balancing stage increases with higher values of β since more DRE is scheduled in the planning stage, which entails higher risks in the scenarios with lower DRE production. On the other hand, the expected

Authorized licensed use limited to: University of Nebraska - Lincoln. Downloaded on July 19,2021 at 19:01:47 UTC from IEEE Xplore. Restrictions apply.

This article has been accepted for inclusion in a future issue of this journal. Content is final as presented, with the exception of pagination.

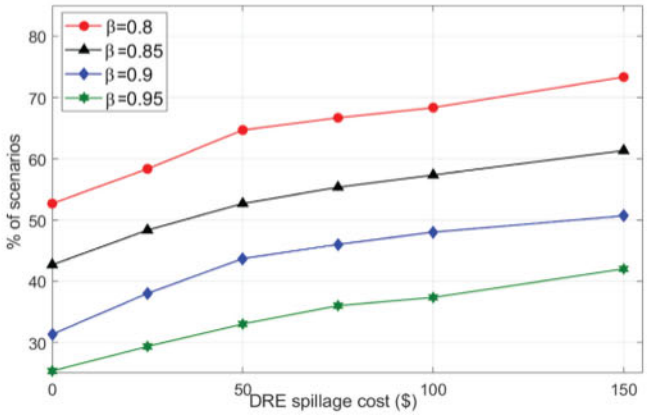

Fig. 7. Impact of the DRE spillage cost in the 12th hour.

TABLE IV
DLMPS IN THE 17TH HOUR WITH BRANCH CONGESTION

Node	1	2	3	4	5	6
DLMP ($/MWh)	41.07	41.07	41.07	41.07	41.07	41.07
Node	7	8	9	10	11	12
DLMP ($/MWh)	41.07	41.07	41.07	41.07	41.07	41.07
Node	13	14	15	16	17	18
DLMP ($/MWh)	41.07	41.07	48.63	48.63	48.63	48.63
Node	19	20	21	22	23	24
DLMP ($/MWh)	41.07	41.07	41.07	41.07	60.52	60.52
Node	25	26	27	28	29	30
DLMP ($/MWh)	60.52	44.31	44.31	44.31	44.31	44.31
Node	31	32	33	-	-	-
DLMP ($/MWh)	44.31	44.31	44.31	-	-	-

downward reserve decreases as β increases since more DRE is utilized in the scenarios with higher DRE production.

To analyze the impact of the DRE spillage cost on the DRE utilization, the risk parameter ε is set to 1, i.e., the chance constraint (22) is neglected. Then, the DRE spillage cost is varied and the percentage of the scenarios N_ω that satisfy the DRE utilization probability in (22) is calculated for different values of β in the 12th hour, as shown in Fig. 7. It turns out that the higher the DRE spillage cost, the higher the number of scenarios that will satisfy the DRE utilization policy. However, high DRE spillage costs may discourage investments in DRE units. On the other hand, the use of DRE utilization constraints with lower DRE spillage costs represents a less risky alternative for DRE producers.

When there is congestion in the distribution network, the DLMPs at the nodes subjacent to the congested branches are higher than the DLMPs at the superjacent nodes since more expensive energy from DDG units needs to be used. Table IV shows the DLMPs at each node of the system during the 17th hour when the branches between nodes 2 and 23, 6 and 26, and 14 and 15 are congested. Note that the DLMPs at all the nodes subjacent to the congested branches are higher than the DLMPs at the nodes not affected by branch congestion.

To illustrate the impact of the DRE uncertainties on the proposed model, the system operation costs obtained from the proposed stochastic optimization model with $N_\omega = 300$ without the DRE utilization constraints are compared with the costs

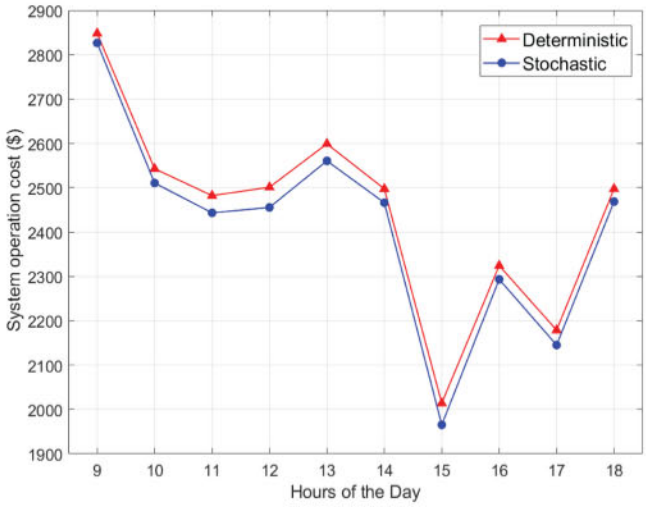

Fig. 8. Expected system operation cost obtained with the stochastic and deterministic models for hours 9–18.

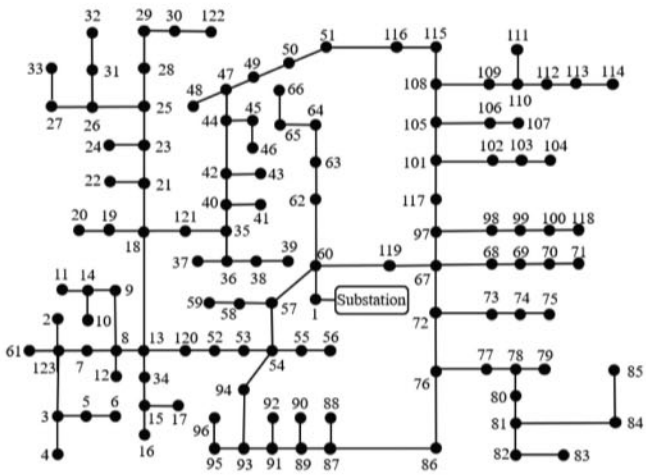

Fig. 9. The 123-node distribution system [42].

obtained from the deterministic counterpart problem that relies on the expected DRE production values rather than considering probabilistic scenarios. The comparison results for hours 9–18 shown in Fig. 8 indicate that the system operation cost can be reduced in all hours when the stochastic nature of DRE is considered in the day-ahead decisions.

C. Results – 123-Node System

In this section, a 123-node system shown in Fig. 9 is used to further verify the applicability of the proposed model for a larger system. The DSE producers are located at nodes 5, 31, 36, 49, 52, 69, 76, 91, 105, and 110. A complete list of all agents at each node of the system and their respective energy and reserve price bids can be found in [41]. The chance-constraint parameters are $\beta = 0.8$ and $\varepsilon = 0.15$. Table V shows the optimality gap, the solution time, and the verification time for N_ω from 10 to 500. Similar to the results of the 33-node system, the optimality gap decreases as the number of scenarios increases. However, compared to the 33-node system, the simulation times for the 123-node system

Authorized licensed use limited to: University of Nebraska - Lincoln. Downloaded on July 19,2021 at 19:01:47 UTC from IEEE Xplore. Restrictions apply.

This article has been accepted for inclusion in a future issue of this journal. Content is final as presented, with the exception of pagination.

TABLE V
OPTIMALITY GAPS AND SIMULATION TIMES FOR DIFFERENT NUMBERS OF DRE SCENARIOS – 123-NODE SYSTEM

$(N_i, N_s, N_{\omega'})$	N_ω	Optimality Gap (%)	Solution Time (s)	Verification Time (s)
(5,5,1500)	10	3.41	0.87	770
	50	1.11	2.07	800
	100	0.79	4.54	862
	200	0.50	20.32	1250
	300	0.36	42.49	1810
	400	0.30	107.85	3425
	500	0.13	156.46	4650

TABLE VI
TOTAL ENERGY AND RESERVE AMOUNTS (MWH) SCHEDULED IN THE PLANNING STAGE – 123-NODE SYSTEM

EG	EFL	EDSE	URPG	URFL	DRPG	DRFL
1,683.2	911.5	310.1	67.2	60.8	68.6	62.4

increase more significantly when a high number of scenarios are considered. The tradeoff between the optimality gap and simulation times should be carefully considered by the DSO. An optimality gap lower than 0.15% was obtained with $(N_i, N_s, N_{\omega'}) = (5, 5, 1500)$ and $N_\omega = 500$, for a 95% confidence interval.

The total amounts of energy and reserve scheduled in the planning stage using the proposed model with $N_\omega = 500$ for the 123-node system are provided in Table VI. In this case, the total reserve amounts are also nearly 40% of the total energy scheduled from DSE units as in the case study for the 33-node distribution system provided in Section IV-B.

V. CONCLUSION

The next-generation retail electricity market will promote increased decentralization, competitiveness, and customer integration, as well as optimize the use of DERs through the effective integration of new entities and market mechanisms in the distribution grid. In this article, a distribution system market clearing and settlement model was presented. The proposed model can help DSOs determine the optimal scheduling of energy and reserve and the DLMPs while considering the DRE production uncertainties at different nodes of the distribution system and different DRE utilization requirements. The resulting problem was formulated as a two-stage chance-constrained stochastic optimization problem, which was solved with an SAA-based Monte Carlo simulation algorithm. Case studies on a 33-node distribution system and a 123-node distribution system showed how different DRE utilization requirements affected the expected system operation cost and the deployment of upward and downward reserves. Moreover, the hourly costs obtained with the proposed stochastic model were compared with the costs obtained with the deterministic counterpart model. The comparison showed that the stochastic model resulted in lower system operation costs for all periods with significant DRE production. Future work can be conducted to study the optimal participation of DER owners in the proposed market clearing mechanism and the correlation of the DSE productions between neighbor nodes. Moreover, the proposed model can also be extended to unbalanced distribution networks for which different solution techniques can be studied and compared.

REFERENCES

[1] E. Commission, "2030 Climate & energy framework," Oct. 2014 [Online]. Available: https://ec.europa.eu/clima/policies/strategies/2030_en.

[2] McKinsey & Company, "Less carbon means more flexibility: Recognizing the rise of new resources in the electricity mix," Oct. 2018 [Online]. Available: https://www.mckinsey.com/industries/electric-power-and-natural-gas/our-insights/less-carbon-means-more-flexibility-recognizing-the-rise-of-new-resources-in-the-electricity-mix

[3] G. Media, "Distributed energy poised for 'explosive growth' on the U.S. grid," Jun. 2018 [Online]. Available: https://www.greentechmedia.com/articles/read/distributed-energy-poised-for-explosive-growth-on-the-us-grid

[4] T.&D. World, "Democratizing energy: The rise of DERs," Jan. 2020. [Online]. Available: https://www.tdworld.com/distributed-energy-resources/article/21120102/democratizing-energy-the-rise-of-ders

[5] J. C. do Prado, W. Qiao, and S. Tomas, "Moving towards distribution system operators: Current work and future directions," in *Proc. IEEE Power Energy Soc. Innov. Smart Grid Technol. Conf.*, Feb. 2019, pp. 1–5.

[6] S. Thomas, "Evolution of the distribution system & the potential for distribution-level markets: A primer for state utility regulators," The National Association of Regulatory Utility Commissioners, Washington, DC, USA, Jan. 2018.

[7] F. A. Rahimi and S. Mokhtari, "Distribution management system for the grid of the future: A transactive system compensating for the rise in distributed energy resources," *IEEE Electrific. Mag.*, vol. 6, no. 2, pp. 84–94, Jun. 2018.

[8] S. Bahramirad, A. Khodaei, and R. Masiello, "Distribution markets," *IEEE Power Energy Mag.*, vol. 14, no. 2, pp. 102–106, Mar./Apr. 2016.

[9] S. Parhizi, A. Khodaei, and S. Bahramirad, "Distribution market clearing and settlement," in *Proc. IEEE Power Energy Soc. Gen. Meeting*, Jul. 2016, pp. 1–5.

[10] S. Parhizi, A. Majzoobi, and A. Khodaei, "Net-zero settlement in distribution markets," in *Proc. IEEE Power Energy Soc. Gen. Meeting*, Jul. 2017, pp. 1–5.

[11] J. Yang *et al.*, "A penalty scheme for mitigating uninstructed deviation of generation outputs from variable renewables in a distribution market," *IEEE Trans. Smart Grid*, vol. 11, no. 5, pp. 4056–4069, Sept. 2020.

[12] M. N. Faqiry, A. K. Zarabie, F. Nassery, H. Wu, and S. Das, "A day-ahead market energy auction for the distribution system operation," in *Proc. IEEE Int. Conf. Electro Inf. Technol.*, May 2017, pp. 182–187.

[13] J. Yang, J. Zhao, J. Qiu, and F. Wen, "A distribution market clearing mechanism for renewable generation units with zero marginal costs," *IEEE Trans. Ind. Informat.*, vol. 15, no. 8, pp. 4775–4787, Aug. 2019.

[14] L. Bai, J. Wang, C. Wang, C. Chen, and F. F. Li, "Distribution locational marginal pricing (DLMP) for congestion management and voltage support," *IEEE Trans. Power Syst.*, vol. 33, no. 4, pp. 4061–4073, Jul. 2018.

[15] M. N. Faqiry, L. Edmonds, H. Zhang, A. Khodaei, and H. Wu, "Transactive-market-based operation of distributed electrical energy storage with grid constraints," *Energies*, vol. 10, no. 11, pp. 1–17, Nov. 2017.

[16] J. Yang, Z. Y. Dong, F. Wen, G. Chen, and Y. Qiao, "A decentralized distribution market mechanism considering renewable generation units with zero marginal costs," *IEEE Trans. Smart Grid*, vol. 11, no. 2, pp. 1724–1736, Mar. 2020.

[17] A. Papavasiliou, "Analysis of distribution locational marginal prices," *IEEE Trans. Smart Grid*, vol. 9, no. 5, pp. 4872–4882, Sept. 2018.

[18] P. Andrianesis, M. Caramanis, R. D. Masiello, R. D. Tabors, and S. Bahramirad, "Locational marginal value of distributed energy resources as non-wires alternatives," *IEEE Trans. Smart Grid*, vol. 11, no. 1, pp. 270–280, Jan. 2020.

[19] S. Hanif, K. Zhang, C. M. Hackl, M. Barati, H. B. Gooi, and T. Hamacher, "Decomposition and equilibrium achieving distribution locational marginal prices using trust-region method," *IEEE Trans. Smart Grid*, vol. 10, no. 3, pp. 3269–3281, May 2019.

[20] A. K. Zarabie, S. Das, and M. N. Faqiry, "Fairness-regularized DLMP-based bilevel transactive energy mechanism in distribution systems," *IEEE Trans. Smart Grid*, vol. 10, no. 6, pp. 6029–6040, Nov. 2019.

[21] A. K. Zarabie and S. Das, "Efficient distributed DSO auction with linearized grid constraints," in *Proc. IEEE Power Energy Soc. Innov. Smart Grid Technol. Conf.*, Feb. 2019, pp. 1–5.

Authorized licensed use limited to: University of Nebraska - Lincoln. Downloaded on July 19,2021 at 19:01:47 UTC from IEEE Xplore. Restrictions apply.

This article has been accepted for inclusion in a future issue of this journal. Content is final as presented, with the exception of pagination.

[22] A. Alassaf, L. Fan, and I. Alsaleh, "Day-ahead distribution market analysis via convex bilevel programming," in *Proc. North Amer. Power Symp.*, Oct. 2019, pp. 1–6.
[23] Z. Li, C. S. Lai, X. Xu, Z. Zhao, and L. L. Lai, "Electricity trading based on distribution locational marginal price," *Int. J. Electric Power Energy Syst.*, vol. 124, no. 1, pp. 1–13, 2021.
[24] M. Jalali, K. Zare, and S. Tohidi, "Designing a transactive framework for future distribution systems," *IEEE Syst. J.*, to be published, doi: 10.1109/JSYST.2020.3022712.
[25] B. S. K. Patnam and N. M. Pindoriya, "DLMP calculation and congestion minimization with EV aggregator loading in a distribution network using bilevel program," *IEEE Syst. J.*, to be published, doi: 10.1109/JSYST.2020.2997189.
[26] J. C. do Prado, H. Vakilzadian, W. Qiao, and D. P. F. Möller, "Stochastic distribution system market clearing and settlement via sample average approximation," in *Proc. North Amer. Power Symp.*, Sept. 2018, pp. 1–6.
[27] M. N. Faqiry, L. Edmonds, H. Wu, and A. Pahwa, "Distribution locational marginal price-based transactive day-ahead market with variable renewable generation," *Appl. Energy*, vol. 259, no. 1, pp. 1–10, Feb. 2020.
[28] R. Mieth and Y. Dvorkin, "Distribution electricity pricing under uncertainty," *IEEE Trans. Power Syst.*, vol. 35, no. 3, pp. 2325–2338, May 2020.
[29] M. E. Baran and F. F. Wu, "Network reconfiguration in distribution systems for loss reduction and load balancing," *IEEE Trans. Power Del.*, vol. 4, no. 2, pp. 1401–1407, Apr. 1989.
[30] Z. Wang, B. Chen, J. Wang, and J. Kim, "Decentralized energy management system for networked microgrids in grid-connected and islanded modes," *IEEE Trans. Smart Grid*, vol. 7, no. 2, pp. 1097–1105, Mar. 2016.
[31] A. Sadeghi-Mobarakeh, A. Shahsavari, H. Haghighat, and H. Mohsenian-Rad, "Optimal market participation of distributed load resources under distribution network operational limits and renewable generation uncertainties," *IEEE Trans. Smart Grid*, vol. 10, no. 4, pp. 3549–3561, Jul. 2019.
[32] Q. Fang, Y. Guan, and J. Wang, "A chance-constrained two-stage stochastic program for unit commitment with uncertain wind power output," *IEEE Trans. Power Syst.*, vol. 27, no. 1, pp. 206–215, Feb. 2012.
[33] P. Rubin, "Choosing big M values," Sep. 2018. [Online]. Available: https://spartanideas.msu.edu/2018/09/17/choosing-big-m-values/
[34] J. M. Morales, A. J. Conejo, H. Madsen, P. Pinson, and M. Zugno, *Integrating Renewables in Electricity Markets*, 1st ed. New York, NY, USA: Springer, 2014, p. 205.
[35] B. K. Pagnoncelli, S. Ahmed, and A. Shapiro, "Sample average approximation method for chance constrained programming: Theory and applications," *J. Optimiz. Theory Appl.*, vol. 142, no. 2, pp. 399–416, Mar. 2009.
[36] PJM interconnection. [Online]. Available: https://www.pjm.com
[37] National solar radiation database. [Online]. Available: https://nsrdb.nrel.gov/
[38] MATLAB econometrics toolbox. [Online]. Available: https://www.mathworks.com/products/econometrics.html
[39] J. Lofberg, "YALMIP: A toolbox for modeling and optimization in MATLAB," in *Proc. IEEE Int. Conf. Robot. Autom.*, Sep. 2004, pp. 284–289.
[40] Using Gurobi with MATLAB. [Online]. Available: https://www.gurobi.com/products/optimization-modeling-language-resources-support/matlab/
[41] IEEE Dataport data set for the 33-node and 123-node distribution systems. [Online]. Available: http://dx.doi.org/10.21227/trjs-r454
[42] IEEE PES test feeders. [Online]. Available: https://site.ieee.org/pes-testfeeders/resources/

Josue Campos do Prado (Member, IEEE) received the B. Eng. degree in electrical engineering from Santa Catarina State University, Joinville, Brazil, in 2012, and the Ph.D. degree in electrical engineering from the University of Nebraska-Lincoln, Lincoln, NE, USA, in 2020.

From October 2018 to July 2020, he conducted research at the Joint Institute for Strategic Energy Analysis of the National Renewable Energy Laboratory. Since August 2020, he has been with Washington State University Vancouver, Vancouver, WA, USA, where he is currently an Assistant Professor with the School of Engineering and Computer Science. His research interests include distributed energy resources, electricity market planning and operation, and optimization under uncertainty applied to power systems.

Wei Qiao (Fellow, IEEE) received the B.Eng. and M.Eng. degrees in electrical engineering from Zhejiang University, Hangzhou, China, in 1997 and 2002, respectively, the M.S. degree in high-performance computation for engineered systems from Singapore-MIT Alliance, Singapore, in 2003, and the Ph.D. degree in electrical engineering from the Georgia Institute of Technology, Atlanta, GA, USA, in 2008.

Since August 2008, he has been with the University of Nebraska–Lincoln, Lincoln, NE, USA, where he is currently a Professor with the Department of Electrical and Computer Engineering. His research interests include renewable energy systems, smart grids, condition monitoring, power electronics, electric motor drives, energy storage systems, and emerging electrical energy conversion devices. He is the author or co-author of more than 260 papers in refereed journals and conference proceedings and holds 11 U.S. patents issued.

Dr. Qiao was a recipient of the 2010 U.S. National Science Foundation CAREER Award and the recipient of the 2010 IEEE Industry Applications Society Andrew W. Smith Outstanding Young Member Award.

Authorized licensed use limited to: University of Nebraska - Lincoln. Downloaded on July 19,2021 at 19:01:47 UTC from IEEE Xplore. Restrictions apply.